

Efficiency of the flagellar propulsion of *Escherichia coli* in confined microfluidic geometriesBen Libberton,^{*} Marie Binz, Harm van Zalinge,[†] and Dan V. Nicolau[‡]*Department of Electrical Engineering and Electronics, University of Liverpool, L69 3GJ Liverpool, United Kingdom*

(Received 9 May 2018; revised manuscript received 22 November 2018; published 9 January 2019)

Bacterial movement in confined spaces is routinely encountered either in a natural environment or in artificial structures. Consequently, the ability to understand and predict the behavior of motile bacterial cells in confined geometries is essential to many applications, spanning from the more classical, such as the management complex microbial networks involved in diseases, biomanufacturing, mining, and environment, to the more recent, such as single cell DNA sequencing and computation with biological agents. Fortunately, the development of this understanding can be helped by the decades-long advances in semiconductor microfabrication, which allow the design and the construction of complex confining structures used as test beds for the study of bacterial motility. To this end, here we use microfabricated channels with varying sizes to study the interaction of *Escherichia coli* with solid confining spaces. It is shown that an optimal channel size exists for which the hydrostatic potential allows the most efficient movement of the cells. The improved understanding of how bacteria move will result in the ability to design better microfluidic structures based on their interaction with bacterial movement.

DOI: [10.1103/PhysRevE.99.012408](https://doi.org/10.1103/PhysRevE.99.012408)**I. INTRODUCTION**

Motile bacteria live in a wide array of environments from the tissues of humans, animals, plants, and abiotic habitats, such as arctic soil, to deep sea vents [1,2]. In many of these environments, bacteria are confined by solid barriers, such as surfaces and obstacles [3–5]. This confinement is either the result of the inherent geometry of the solid environment or the result of the bacteria themselves, which can build complex colonies, known as biofilms [6]. Biofilms have been shown to comprise many complex, biologically made, microstructures, one example being the formation of channels, which direct the flow of nutrients to the biofilm, as well as restricting the movement of bacteria [7,8]. Regardless of the source of the confinement, bacterial motility, which is an essential instrument for growth and survival, has been shown to exhibit important differences when bacteria move in volumes with sizes similar to their cells as opposed to the motility non-confined spaces [9,10]. For instance, when *Escherichia coli* (*E. coli*) form a biofilm on an agar plate, the upper part of the swarm is stationary, and the underside moves [11]. From the applications point of view, many bacteria are medically or industrially relevant. As these artificial environments usually contain restricted geometries, it is of vital importance that we understand the bacterial behavior in confining spaces and, subsequently, be able to control or to mitigate their deleterious effects or, conversely, elicit beneficial ones. For example, certain bacteria which live in confined habitats are clinically relevant, such as pyelonephritis in the kidney [1]

or bloodstream infections where many capillaries are less than 10 μm in diameter [12]. In other cases the bacteria are industrially relevant, such as using bacteria as motile biosensors [13] and in microbial fuel cells [14]. Finally, a biocomputation approach has been proposed [15] and recently demonstrated [16], which consists of using motile biological entities, including bacteria, as a large number of agents exploring microfluidic networks encoding a difficult mathematical problem. As the advances in microfabrication have made it possible to construct microstructures of similar dimensions as those found in naturally occurring restricted geometries, this development has opened new avenues in the study of bacteria while they are confined in structures similar in size to those they naturally encounter [17,18]. For instance, complex structures can be used to entrap individual bacteria and study their behavior, physiology, or gene expression [19,20]. The most commonly used material to fabricate the confining structures is polydimethylsiloxane (PDMS), which remains popular due to its biocompatibility, transparency, and its permeability to oxygen [21]. Also the manufacturing of microstructures made of PDMS does not require high temperatures or specialized equipment [22]. Several studies have reported a variety of behaviors of motile bacteria in confined geometries [2,9,23–27]. These studies have focused mainly on flagellar motility, which is the most common propulsion system. Flagella are motors that protrude from the bacterial surface and rotate in order to propel the bacterial cells forward [28–30]. It was shown that *E. coli* has a preference to swim on the right hand side of channels [24]. In addition it has been shown that the trajectory and velocity of *Serratia marcescens* varies depending on the channel width and the complexity of the geometry [23]. Motile bacteria have even been shown to traverse channels that are narrower than themselves although the mechanism to achieve this is significantly different from standard, flagella mediated swimming [10]. In this paper, we examine the swimming characteristics of the flagellate

^{*} Also at MAX IV Laboratory, Lund University, Lund, Sweden.[†] vzalinge@liverpool.ac.uk[‡] Also at Department of Bioengineering, McGill University, Montreal, Quebec H3A 0C3, Canada. Electronic address: dan.nicolau@mcgill.ca

bacterium *E. coli* in micron-sized channels. We investigate how restricting the geometry within which the bacterium is moving influences its velocity and the preferential location of individual cells with regard to the channel wall. Although it is widely reported that bacteria adhere to the walls, there is no information on the optimum distance between cell and wall at which the proximity enhances the motility of the bacterium. Although this information can be relevant for a large number of applications, from medical to industrial, it is particularly important for the precise design of microfluidics devices using motile bacteria.

II. MATERIALS AND METHODS

A. Bacterial culture conditions

E. coli strain MC1061 was cultured in Luria-Bertani (LB) broth (LabM). Midexponential cultures were prepared by diluting an overnight culture 1:100 and allowing the bacterial population to grow at 37 °C while shaking at 200 rpm until reaching an optical density (600 nm) of ~ 0.5 .

B. Preparation of PDMS channels

A silicon master was prepared using photolithographic techniques followed by deep reactive ion etching using the Bosch recipe [31]. The channels were generated by replica molding of the master with PDMS. The PDMS precursor and curing agent (Sylgard 184, Dow Corning, MI, USA) were mixed in a 10:1 ratio. The mixture was then degassed under vacuum and poured over the silicon master before being heat cured for 12 h at 65 °C. After curing, the PDMS structure was carefully peeled away. Prior to use, the PDMS structure was made hydrophilic by UV treatment before being attached to an oxidized glass microscope slide which formed the base of each channel. Prior to inoculation, the PDMS structures were filled with a solution containing bovine serum albumin (BSA) by placing the samples in a vacuum chamber with the structures submerged in the BSA solution. This step was performed to block any surface acting component in the channels. The BSA was then removed using filter paper to draw the liquid out of the channels. The channels were then refilled with LB liquid broth using the same method. A 10 μ l culture of cells (OD600 of 0.5) were loaded directly into the PDMS structures through the open edges.

C. Image acquisition and analysis

E. coli cells were observed in the channels at room temperature. The microscope slide with the PDMS structures was placed on the stage of a Leica DM LB2 upright microscope. Video images were captured using 40 \times bright field objectives, a 1.5 \times or 2 \times magnification changer, and a Spot camera (Diagnostic Instruments, Inc., USA) that collected images at 8.33 frames per second. The videos were analyzed and cells tracked using IMAGEJ with the plug-in MTRACK. All bacterial movement was directionality normalized so that all trajectories of the bacteria were moving in the same direction.

III. RESULTS AND DISCUSSION

A. The speed of *E. coli* is modulated by channel geometry

To examine how confined geometries affect the swimming velocity of *E. coli* cells, capped channels ranging in width from 2 to 10 μ m, filled with LB medium, were used (Fig. 1 and Table S1 in the Supplemental Material [32]). The height of both the channels and the 100 \times 100 μ m² plaza was 10 μ m. *E. coli* cells were introduced into a “plaza” at the entrance to each of the channels and bacterial cells were allowed to enter by self-propelled motion. The statistical analysis was performed on, at least, 30 different bacterial cells for each confining geometry, taken from, at least, three different sets of experiments. Each bacterial cell was tracked for between 1 and 10 s while moving, thus generating a total of between 300 and 1000 velocity data points that contain useful information on each structure. The strain of *E. coli* (MC1061) moves in a run and tumble manner, i.e., the run, a period of unidirectional travel, the run in which the flagella are cooperating with each other; followed by the tumble, a short period in which the symmetry of the flagella is broken and the forward motion changes into a rotational movement [28]. It has been shown that the presence of a solid surface will significantly suppress the occurrence of tumbling [33]. Additionally, while inside the narrow channels, the tumbling events might still be occurring, and they, or the resulting change in direction, cannot be observed due to the geometrical restrictions of the channel.

In order to be able to compare the hindered and nonhindered motility of the bacteria, the movement in the plaza area is used as a control to characterize the free movement. Within the plaza it can be observed (Fig. S1, Supplemental Material [32]) that there are a large number of nonmotile bacteria. When ignoring these stationary bacteria, the mean velocity was $(12 \pm 6) \mu\text{m s}^{-1}$. Although the experimental conditions are different, the velocities observed here are not dissimilar to those observed elsewhere [34,35].

The bacteria that move within the confinement of a channel travel faster than those in the plaza (Fig. 2). For example, when bacteria entered the 10 μ m channel, the average velocity increased to $(23 \pm 1) \mu\text{m s}^{-1}$, and there were far fewer

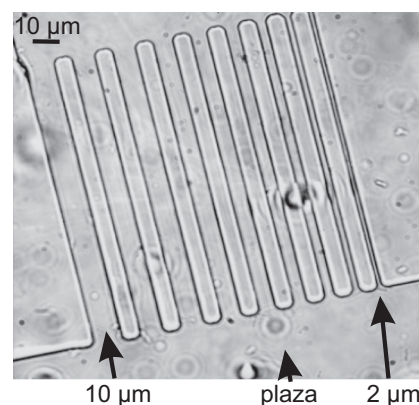


FIG. 1. Microscopic image of the channel structure with the plaza at the top and bottom of the image. The channels range from 2 μ m on the right to 10 μ m on the left.

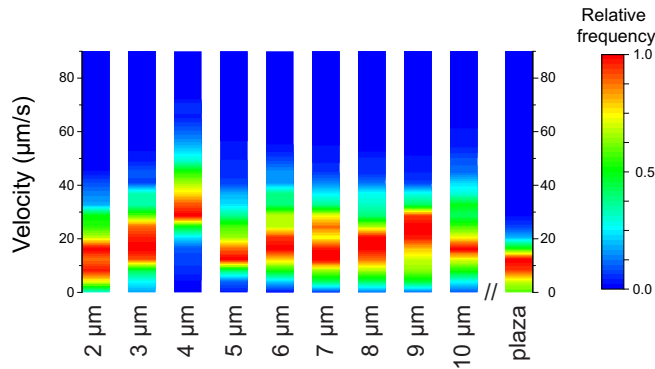


FIG. 2. Relative frequency, normalized to the most occurring velocity in that channel, of the velocity of *E. coli* in the different channel widths as well as in the plaza.

stationary cells (Fig. 2, and Supplemental Material [32]). The velocity in the channels of $5 \mu\text{m}$ and wider was relatively constant at approximately $(21 \pm 11) \mu\text{m s}^{-1}$. The average velocity of the bacteria in the three narrowest channels remained constant, apart from the $4 \mu\text{m}$ channel where the highest average velocity was observed, i.e., $(37 \pm 11) \mu\text{m s}^{-1}$. The increase in the velocity in $4 \mu\text{m}$ wide channels is probably caused by the propulsive advantage of swimming near a wall and show improvement that is comparable to that predicted before [36]. The decrease in the average velocity in the $2 \mu\text{m}$ channel is similar to the behavior observed elsewhere, attributed to the disruption to the bacteria due to the close proximity of the wall [9].

The profile of the velocity distribution changes depending on the channel width (Supplemental Material, Fig. S1 [32]). The distributions of velocity in the wider channels ($8 \mu\text{m}$ width and wider) tend to be narrower, steeper, and less symmetric as the tail towards higher velocities is larger. In the narrower channels, i.e., between 2 and $5 \mu\text{m}$, the distributions are also not completely symmetric, but they are broader, indicating that more bacterial cells move at similar velocities. Interestingly, only the $4 \mu\text{m}$ channel shows a Gaussian type of distribution. This shows that, by changing the cross section of a channel, it is possible to influence the overall behavior of an entire population of *E. coli* cells.

B. *E. coli* swim preferentially at the sides of channels

In order to determine the location of *E. coli* in the geometric structures, the position of every recorded bacterial cell, defined as the center of the cell body, was calculated with respect to the walls of the channel. The location of the bacterium has been defined as the center of the cell body. In the narrower structures, i.e., 2 – $4 \mu\text{m}$ wide, the cells are more likely to be found at the center of the channel (see Fig. 3 and Supplemental Material Fig. S2 [32]). Although located predominantly at the center, there is a skew in the distribution to the right indicating that bacteria in the $3 \mu\text{m}$ channel tend to swim more often on the right hand side of the channel as observed elsewhere [24]. In the $5 \mu\text{m}$ channel a bimodal distribution of cells becomes apparent with fewer cells being found in the middle of the channel and more being found closer to the walls on either side. This trend amplifies as the

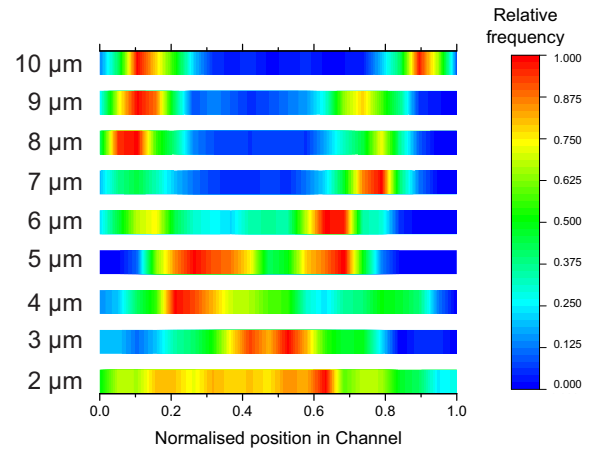


FIG. 3. Relative frequency of the position perpendicular to the long axis of the various channels with the position normalized with respect to the channel width.

width of the channels increases to the extent that in the $10 \mu\text{m}$ channels nearly all bacterial cells are located close to the sides of the channel. The distribution of the cells at either the left or the right hand side is even in the 10 and $5 \mu\text{m}$ channels. However, in the 9 and the $8 \mu\text{m}$ channels the bacteria tend to be located more on the left hand side wall, and in the 7 and $6 \mu\text{m}$ channels they tend to be slightly more located on the right hand side wall. These findings suggest that the swimming preferences of the bacterial cells are modulated by the geometry of the swimming environment and that in wider channels, bacteria tend to swim in straight motility patterns and close to the walls.

The actual separation between the wall and the bacterial cells ranges between 1 and $2 \mu\text{m}$. As the size of the *E. coli* cell is on the order of 0.5 – $1 \mu\text{m}$, it is to be expected that the two distributions at either wall will merge in the $4 \mu\text{m}$ wide channels [37]. The propensity of the bacteria to adhere to the channel walls is caused by the combination of hydrodynamic effects and steric interactions and dominated by near-field coupling between cells and the wall [38].

C. Channel width simultaneously affects the velocity and the location of bacteria

In the narrowest channels, *E. coli* cells swim mainly in the middle of the channel with the fastest cells being present along the median line [Fig. 4(a)]. However, in channels with widths of $5 \mu\text{m}$ and above, the populations of bacteria move preferentially towards the sides of the channels and are rarely observed in the center [Fig. 4(b)]. Interestingly, the fastest moving cells are also found towards the edges of the channels and not towards the center, indicating that the vicinity of the channels does not decrease the swimming velocity but rather counterintuitively amplifies it. There are a number of effects that will cause the velocity of the bacteria to increase near the channel wall. The first are the hydrodynamic effects the wall have on the movement of the bacteria [39]. Second, it has been shown that faster moving bacteria have the ability to remove slower moving ones from the wall [40]. Third, cells close to the channel wall will create strong fluid flows against

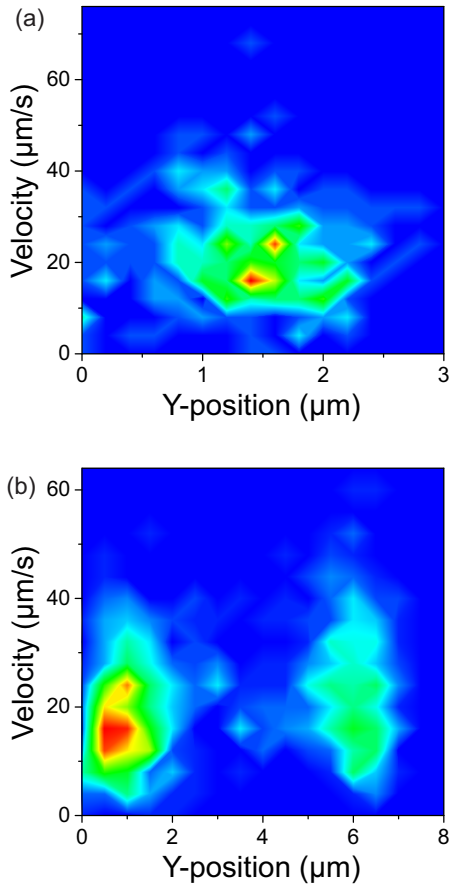


FIG. 4. The normalized two dimensional histogram of the velocity of the cells and the position perpendicular (Y position) to the channel's long side for (a) the $3 \mu\text{m}$ (325 event) and (b) the $8 \mu\text{m}$ (787 events) wide channel.

the direction of travel in their vicinity causing a reduction of the speed in the center of the channel [41,42]. In addition, it has been shown that the hydrodynamic interaction between the wall and the bacterium causes the cell to remain in close proximity for a prolonged period of time [43], thus, causing a reduction of the tumbling probability.

D. Efficiency of the flagellar propulsion of *E.coli* is modulated by the width of the microfluidic channels

The observed distribution of bacterial velocity and position in confined channels can be explained by the variation of the interaction between the flagella and the wall. To propel the bacterial cell forward, the flagella exert a mechanical force, and some of this energy will be dissipated within the surrounding media. By confining the motility within a channel, more of the energy generated by the flagella will be used to propel the bacterial cell, including by pushing against the walls, leading to an increase in velocity. This conclusion is supported by the average velocity data (Fig. 2). For instance, in the plaza the cells move at $(12 \pm 6) \mu\text{m s}^{-1}$, and in wider channels where the cells preferentially move close to one wall, the effect is less efficient but still an improvement compared to the plaza, i.e., the cells accelerate to $(21 \pm 11) \mu\text{m s}^{-1}$. The optimal motility from the average velocity point of view, is

the channels with widths of $4 \mu\text{m}$ channel where the velocity increases to $(37 \pm 11) \mu\text{m s}^{-1}$. However, in even narrower channels, the proximity of the walls will start to severely interfere with the functioning of the flagella, which results in a decrease in the velocity. Furthermore, the bacteria appear to move preferentially in a region approximately $1.5 \mu\text{m}$ away from the side walls. Moreover, these cells show the highest velocities with a reduction in velocity once they are further away from the walls. This suggests that the optimum interaction distance between the flagella of *E. coli* and a solid structure is $1.5 \mu\text{m}$.

E. Hydrostatic potential

As mentioned previously, one of the potential causes for the observed behavior can be found in the hydrostatic potential. This dictates the location of the *E. coli* cells inside a microfluidic structure [44]. This potential can be described by the Lennard-Jones formalism,

$$U_w = 4k_B T \left\{ \left(\frac{\sigma}{r} \right)^{12} - \left(\frac{\sigma}{r} \right)^6 \right\}, \quad (1)$$

where k_B represents the Boltzmann constant, T represents the temperature, and r represents the separation between the wall and the bacterium. σ is related to the location of the potential minimum r_m via $r_m = 2^{(1/6)}\sigma$. For those channel widths in which two clear populations can be distinguished, it is possible to use their separation with the channel to the wall to determine the location of the minima. Using the distances provided in Table S1 of the Supplemental Material [32], the experimentally determined value for $r_m = (1.2 \pm 0.2) \mu\text{m}$. The minimum is also related to the dimensions of the bacterial cell [45]. Using the data for the broadest channel in the simulation, the optimum separation between the wall and the cell is approximately $17a$, where a is a parameter related to the dimensions of the cell. With this parameter the estimated diameter of the *E. coli* cell is $(0.6 \pm 0.1) \mu\text{m}$, whereas the length is $(4.4 \pm 0.7) \mu\text{m}$. These values are within range of the dimensions of an *E. coli* swarmer cell, diameter $0.8 \mu\text{m}$ and length $6 \mu\text{m}$ [44].

When the experimentally determined potential minimum is taken into account, the Lennard-Jones potential as a function of the location in the channel can be determined [see Fig. 5(a)]. It has to be noted that there is an additional potential due to the presence of the top and bottom of the channel. The distance between them is constant and sufficiently large. Consequently, they are solely responsible for maintaining the cellular movement on a single plane. For this reason, they are ignored in the further interpretation of the results. When the wall separation becomes approximately $4 \mu\text{m}$, the two potentials begin to overlap [Fig. 5(b)]. The consequence of this overlap is a deeper minimum but also a reduced energy barrier the cells have to overcome to move perpendicular to the wall. In effect, there exists a very broad minimum for the cells to move in, which facilitates the movement when the bacteria encounter slight variations in the exact location of the walls. The overall effect will be that bacterial cells are spread out throughout the channel but also have less hindered movement shown by an increase in their velocity. When the channel becomes narrower, the overlap becomes larger until,

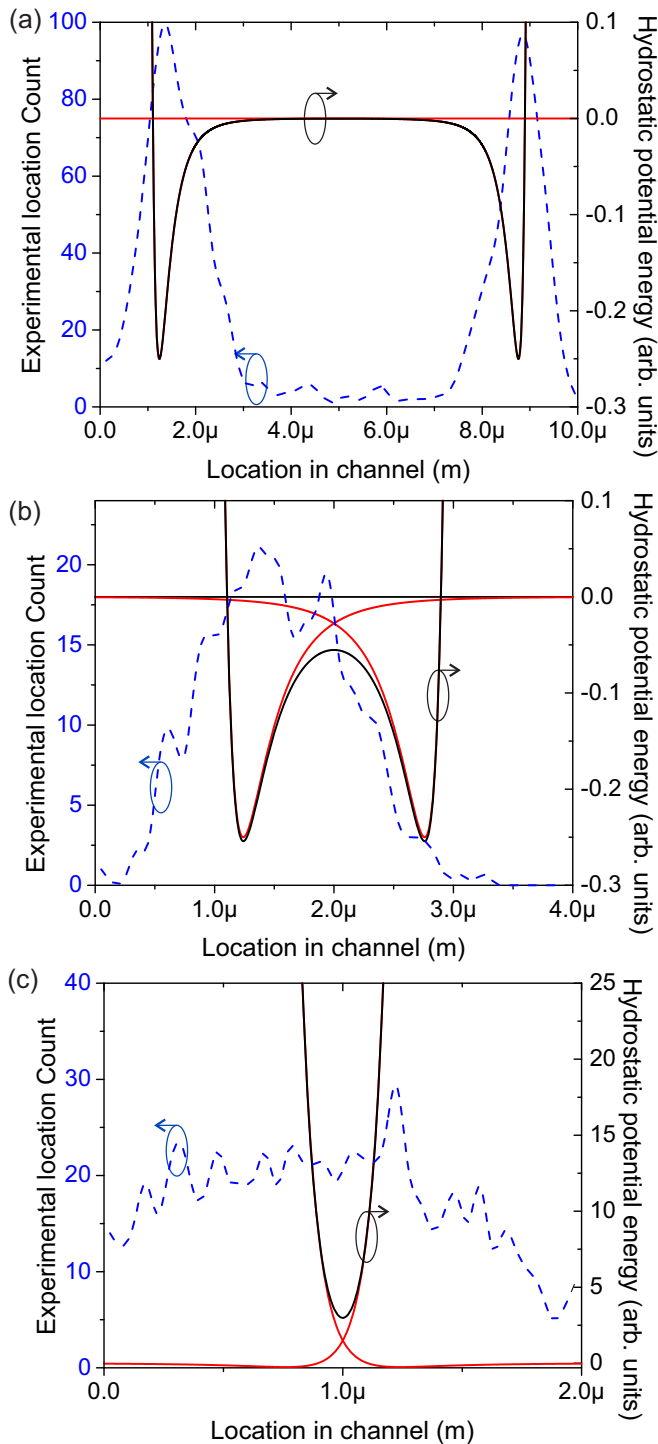


FIG. 5. The experimentally determined cell location (dashed, blue curve) and the hydrostatic potential (solid, black curve), the red lines indicate the contributions from the individual walls as a function of the location within the channel for (a) a $10\ \mu\text{m}$, (b) $4\ \mu\text{m}$, and (c) $2\ \mu\text{m}$ wide channel.

once again, a single channel is formed [Fig. 5(c)]. With infinitely high potential barriers on either side, the bacteria

will move in this single channel. However, small variations in the width of the channel will form large energy barriers for the cells to overcome, which leads to a reduction of the motility.

The main conclusion of this analysis is that, when swimming through channels, *E. coli* cells tend to swim close to the walls. This finding can have important medical implications where many infections caused by *E. coli* occur in restricted geometries. Understanding how motility is affected in such clinically relevant environments could suggest better treatments or the development of new therapeutic compounds aimed at inhibiting the virulence of infecting microbes [46]. For any artificial device that requires the movement of bacteria, e.g., laboratory on a chip, there are certain design parameters that are critical for the correct functioning. Taking the example of cell selection devices for *E. coli*, the results suggest that channels of $4\ \mu\text{m}$ width should be used if speed is the key performance parameter, but smaller widths, e.g., around $2\ \mu\text{m}$, would minimize the effect of the tumbling of bacteria, therefore improving their unidirectional motility and thus decrease selection errors. Although this paper suggested some simple design rules, further experimental and simulation work will be required for the optimization of more complex structures, such as logic junctions, and rectifiers.

IV. CONCLUSION

We have shown that fine variations of the widths of linear microfluidic channels hosting the motility of *E. coli* have large impacts on its average velocity and the positioning laterally in the channels. Rather counterintuitively, channels with smaller widths appear to increase the average velocity of bacteria with a maximum effect around $4\ \mu\text{m}$ for which an approximately threefold amplification of the velocity has been observed. This effect is caused by the optimum interaction distance between the walls and the flagella of the bacterium and hydrostatic potential caused by the proximity of the channel wall. Narrower widths of the channel would, however, have a deleterious effect on velocity due to the strong interactions between the walls and the flagella. This paper suggests some simple design rules, such as the use of $4\ \mu\text{m}$ channels if speed is of the key operational parameter of the device, and the use of $\sim 2\ \mu\text{m}$ channels to reduce the effects of tumbling. Further experimental and simulation work will be required for the optimization of more complex structures, such as logic junctions, and rectifiers.

ACKNOWLEDGMENTS

The work presented here was financially supported by the European Union Seventh Framework Programme (Programme No. FP7/2007-2011) under Grant Agreement No. 228971 (MONAD) and by the Defence Advanced Research Projects Agency (DARPA) under Grant Agreement No. HR0011-16-2-0028.

- [1] K. Melican, R. Sandoval, A. Kader, L. Josefsson, G. Tanner, B. Molitoris, and A. Richter-Dahlfors, *PLoS Pathog.* **7**, e1001298 (2011).
- [2] L. Ping, V. Wasnik, and E. Emberly, *FEMS Microbiol. Ecol.* **91**, 1 (2015).
- [3] L. Chao and B. Levin, *Proc. Natl. Acad. Sci. USA* **78**, 6324 (1981).
- [4] B. Libberton, M. Horsburgh, and M. Brockhurst, *Evol. Appl.* **8**, 738 (2015).
- [5] G. Rosenber, N. Steinberg, Y. Oppenheimer-Shaanan, T. Olender, S. Doron, J. Ben-Ari, A. Sirota-Madi, Z. Bloom-Ackermann, and I. Kolodkin-Gal, *npj Biofilms Microbiomes* **2**, 15027 (2016).
- [6] J. Costerton, P. Stewart, and E. Greenberg, *Science* **284**, 1318 (1999).
- [7] E. Banin, M. Vasil, and E. Greenberg, *Proc. Natl. Acad. Sci. USA* **102**, 11076 (2005).
- [8] J. Wilking, V. Zaboradaev, M. De Volder, R. Losick, M. Brenner, and D. Weitz, *Proc. Natl. Acad. Sci. USA* **110**, 848 (2013).
- [9] S. Biondi, J. Quinn, and H. Goldfine, *AIChE J.* **44**, 1923 (1998).
- [10] J. Männik, R. Driessen, P. Galajda, J. Keymer, and C. Dekker, *Proc. Natl. Acad. Sci. USA* **106**, 14861 (2009).
- [11] R. Zhang, L. Turner, and H. Berg, *Proc. Natl. Acad. Sci. USA* **107**, 288 (2010).
- [12] C. Hall, C. Reynell, B. Gesslein, N. Hamilton, A. Mishra, B. Sutherland, F. O'Farrell, A. Buchan, M. Lauritzen, and D. Attwell, *Nature (London)* **508**, 55 (2014).
- [13] E. Steager, M. Sakar, D. Kim, V. Kumar, G. Pappas, and M. Kim, *J. Micromech. Microeng.* **21**, 035001 (2011).
- [14] H. W. Harris, M. Y. El-Naggar, O. Bretschger, M. J. Ward, M. F. Romine, A. Y. Obraztsova, and K. H. Nealon, *Proc. Natl. Acad. Sci. USA* **107**, 326 (2010).
- [15] D. Nicolau, D. Nicolau Jr., G. Solana, K. Hanson, L. Filippini, L. Wang, and A. Lee, *Microelectron. Eng.* **83**, 1582 (2006).
- [16] J. Nicolau, D. V., M. Lard, T. Korten, F. Van Delft, M. Persson, E. Bengtsson, A. Månsson, S. Diez, and H. Linke, *Proc. Natl. Acad. Sci. USA* **113**, 2591 (2016).
- [17] F. Hol and C. Dekker, *Science* **346**, 1251821 (2014).
- [18] D. Weibel, W. DiLuzio, and G. Whitesides, *Nat. Rev. Microbiol.* **5**, 209 (2007).
- [19] M. Khorshidi, P. Rajeswari, C. Wählby, H. Joensson, and H. Andersson Svahn, *Lab Chip* **14**, 931 (2014).
- [20] J. Ryley and O. Pereira-Smith, *Yeast* **23**, 1065 (2006).
- [21] S. Sia and G. Whitesides, *Electrophoresis* **24**, 3563 (2003).
- [22] J. Connell, E. Ritschdorff, M. Whiteley, and J. Shear, *Proc. Natl. Acad. Sci. USA* **110**, 18380 (2013).
- [23] M. Binz, A. Lee, C. Edwards, and D. Nicolau, *Microelectron. Eng.* **87**, 810 (2010).
- [24] W. DiLuzio, L. Turner, M. Mayer, P. Garstecki, D. Weibel, H. Berg, and G. Whitesides, *Nature (London)* **435**, 1271 (2005).
- [25] E. Lauga, W. DiLuzio, G. Whitesides, and H. Stone, *Biophys. J.* **90**, 400 (2006).
- [26] S. Van Teeffelen, U. Zimmermann, and H. Löwen, *Soft Matter* **5**, 4510 (2009).
- [27] J. E. Sosa-Hernández, M. Santillán, and J. Santana-Solano, *Phys. Rev. E* **95**, 032404 (2017).
- [28] H. Berg and R. Anderson, *Nature (London)* **245**, 380 (1973).
- [29] G. Wadhams and J. Armitage, *Nat. Rev. Mol. Cell Biol.* **5**, 1024 (2004).
- [30] S. Bianchi, F. Saglimbeni, A. Lepore, and R. Di Leonardo, *Phys. Rev. E* **91**, 062705 (2015).
- [31] K. Hanson, D. Nicolau, Jr., L. Filippini, L. Wang, A. Lee, and D. Nicolau, *Small* **2**, 1212 (2006).
- [32] See Supplemental Material at <http://link.aps.org/supplemental/10.1103/PhysRevE.99.012408> for additional statistical information.
- [33] M. Molaei, M. Barry, R. Stocker, and J. Sheng, *Phys. Rev. Lett.* **113**, 068103 (2014).
- [34] N. Darnton, L. Turner, S. Rojevsky, and H. Berg, *J. Bacteriol.* **189**, 1756 (2007).
- [35] A. Patteson, A. Gopinath, M. Goulian, and P. E. Arratia, *Sci. Rep.* **5**, 15761 (2015).
- [36] M. Ramia, D. Tullock, and N. Phan-Thien, *Biophys. J.* **65**, 755 (1993).
- [37] G. Reshes, S. Vanounou, I. Fishov, and M. Feingold, *Biophys. J.* **94**, 251 (2008).
- [38] S. Bianchi, F. Saglimbeni, and R. Di Leonardo, *Phys. Rev. X* **7**, 011010 (2017).
- [39] M. Theves, J. Taktikos, V. Zaboradaev, H. Stark, and C. Beta, *Europhys. Lett.* **109**, 28007 (2015).
- [40] A. Costanzo, J. Elgeti, T. Auth, G. Gompper, and M. Ripoll, *Europhys. Lett.* **107**, 36003 (2014).
- [41] H. Wioland, E. Lushi, and R. Goldstein, *New J. Phys.* **18**, 075002 (2016).
- [42] N. Figueroa-Morales, G. L. Miño, A. Rivera, R. Caballero, E. Clément, E. Altshuler, and A. Lindner, *Soft Matter* **11**, 6284 (2015).
- [43] K. Drescher, J. Dunkel, L. Cisneros, S. Ganguly, and R. Goldstein, *Proc. Natl. Acad. Sci. USA* **108**, 10940 (2011).
- [44] J.-M. Swiecicki, O. Sliusarenko, and D. B. Weibel, *Integr. Biol.* **5**, 1490 (2013).
- [45] T. Eisenstecken, J. Hu, and R. Winkler, *Soft Matter* **12**, 8316 (2016).
- [46] Q. Guo, Y. Wei, B. Xia, Y. Jin, C. Liu, X. Pan, J. Shi, F. Zhu, J. Li, L. Qian, X. Liu, Z. Cheng, S. Jin, J. Lin, and W. Wu, *Sci. Rep.* **6**, 19141 (2016).